HAL
open science

Robust Simulation for Hybrid Systems Chattering Path Avoidance

Ayman Aljarbouh, Benoît Caillaud

To cite this version:

Ayman Aljarbouh, Benoît Caillaud. Robust Simulation for Hybrid Systems Chattering Path Avoidance. The 56th Conference on Simulation and Modelling (SIMS 56), Linköping University, Oct 2015, Linköping, Sweden. pp.175-185, 10.3384/ecp15119175 . hal-01247074v4

HAL Id: hal-01247074

https://hal.science/hal-01247074v4

Submitted on 12 Jan 2016

HAL is a multi-disciplinary open access archive for the deposit and dissemination of scientific research documents, whether they are published or not. The documents may come from teaching and research institutions in France or abroad, or from public or private research centers.

L'archive ouverte pluridisciplinaire **HAL**, est destinée au dépôt et à la diffusion de documents scientifiques de niveau recherche, publiés ou non, émanant des établissements d'enseignement et de recherche français ou étrangers, des laboratoires publics ou privés.

Copyright

Robust Simulation for Hybrid Systems:
Chattering Path Avoidance

Ayman ALJARBOUH[1] Benoit CAILLAUD[1]

[1]INRIA/IRISA Rennes, Campus de Beaulieu, 35042 Rennes Cedex, France,
{ayman.aljarbouh,benoit.caillaud}@inria.fr

Abstract

The sliding mode approach is recognized as an efficient tool for treating the chattering behavior in hybrid systems. However, the amplitude of chattering, by its nature, is proportional to magnitude of discontinuous control. A possible scenario is that the solution trajectories may successively enter and exit as well as slide on switching manifolds of different dimensions. Naturally, this arises in dynamical systems and control applications whenever there are multiple discontinuous control variables. The main contribution of this paper is to provide a robust computational framework for the most general way to extend a flow map on the intersection of p intersected $(n-1)$-dimensional switching manifolds in at least p dimensions. We explore a new formulation to which we can define unique solutions for such particular behavior in hybrid systems and investigate its efficient computation/simulation. We illustrate the concepts with examples throughout the paper.
Keywords: Hybrid systems, Non-smooth dynamical systems, Discontinuity mappings, Chattering-free simulation, Numerical methods.

1 Introduction

Hybrid systems are heterogeneous dynamical systems exhibiting both continuous and discrete dynamics. Systems of this type arise naturally in control systems where the value of a control variable may jump or whenever the laws of physics are dicontinuous. They are common in a wide variety of engineering applications dealing with multi-modal systems such like mechanical systems with impact phenomena, robotics, mechatronics, automotive industry, power systems, process control, as well as embedded computation where program codes interact with the physical world (Zhang et al., 2001; Cai et al., 2007). In such dynamical systems, the state variables are capable of evolving continuously (flowing) and/or evolving discontinuously (jumping) (Cai et al., 2007). The dynamical behavior characterized by interacting continuous variables and discrete switching logics can be captured by a mathematical framework given in terms of time-driven continuous variable dynamics (usually described by differential or difference equations) and event-driven discrete logic dynamics (whose evolutions depend on "if-then-else " type of rules and may be described by automata) (Lin and Antsaklis, 2009).
Such interaction of continuous-time and discrete-time dynamics may lead to an infinitely fast and continuous switching between several dynamics, such behavior is called a *chattering* behavior (Zhang et al., 2008). This often occurs in the optimal control of continuous and hybrid systems. Chattering executions can be defined as solutions to the hybrid system having infinitely many discrete transitions in finite time. Such behavior can be intuitively thought of as *involving infinitely fast switching among different control actions or modes of operation*. Similar behavior appears in variable structure control systems and in relay control systems (Johansson et al., 2002). The numerical simulation of hybrid systems exhibiting a chattering behavior appears to come to a halt, since infinitely many transitions would need to be simulated. This requires high computational costs as small step-sizes are required to maintain the numerical precision. Chattering behavior has to be treated in an appropriate way to ensure that the numerical integration progress in a reasonable time. This has been investigated by means of different methods. In general, one may prevent the chattering in hybrid systems by inducing a smooth sliding motion on the switching manifold on which the chattering occurs (di Bernardo et al., 2008; Weiss et al., 2014; Guardia et al., 2011). While the infinitely fast switching between modes occurs, a smooth motion along the switching surface may emerge while eliminating the fast chattering. Differential inclusions (DIs) of the Filippov type (the so-called equivalent dynamics) can be used to define a regularized solution trajectory in a small neighborhood of the switching manifold on which the chattering occurs so that the average velocity of sliding on the surface can be determined (Filippov, 1988; Biák et al., 2013). Another approach (the so-called equivalent control) was proposed by Utkin (Utkin, 1992). However, the computation of the equivalent dynamics turns of to be difficult whenever the systems chat-

ters between more than two dynamics. One of the main properties of chattering behavior is that the solution trajectory may successively enter and exit as well as slide on switching manifolds of different dimensions. Problems with this type of sliding arise naturally in dynamical systems and control applications whenever there are multiple discontinuous control variables. Such multiple sliding behavior may be the origin of non-uniqueness of solution as an inescapable and important property of heterogeneous dynamical systems with discontinuous control variables.
The main contribution of this paper is to provide an adequate technique to detect chattering "on the fly" in real-time simulation and compute its regularization beyond the infinitely fast mode switching. In particular, we present a robust and computationally efficient framework for the most general case of p intersected switching manifolds, as well as the extent of how unique solutions in such cases can be defined. A hierarchical application of convex combinations to form a differential inclusion on the intersection is employed. We provide a novel computational framework which treats non-smoothness in the trajectory of the state variables during the regularization of chattering by a smooth correction after each integration time-step. The paper is organized as follows: Section 2 provides preliminaries on the modeling of hybrid systems. Section 3 deals with the chattering behavior as well as the chattering on switching intersection. Section 4 presents a numerical approach to integrate the system dynamics while eliminating the fast switching. Finally, simulation results and conclusion of the study are given in Sections 5 and 6, respectively.

2 Modeling of Hybrid Systems

Definition 1: **(Hybrid Automaton)**
A hybrid automaton HA is a collection $HA = (Q, X, Init, f, I, E, G, R)$, wehre

1. Q, a finite set of discrete states $q \in Q$.
2. X, a finite set of continuous states variables $x_i \in X$.
3. $Init \subseteq Q \times X$, is a finite set of initial states.
4. $f : Q \times \mathbb{R}^n \to \mathbb{R}^n$, is a flow map, which describes, through a differential equation, the continuous evolution of the continuous state variable x.
5. I: $Q \rightrightarrows \mathbb{R}^n$, assigns to each location $q \in Q$ an invariant map, which describes the conditions that the continuous state x has to satisfy at this mode.
6. $E \subset Q \times Q$, is a collection of discrete transitions, which identifies the pairs (q, q') such that a transition from the mode q to the mode q' is possible.
7. $G : E \rightrightarrows \mathbb{R}^n$, assign to each $e = (q, q') \in E$ a guard to which the continuous state x must belong so that a transition from q to q' can occur.
8. $R : E \times \mathbb{R}^n \to \mathbb{R}^n$ assign to each $e = (q, q') \in E$ and $x \in X$ a reset map $R(e, x)$, which describes, for each $e = (q, q') \in E$, the value to which the continuous state $x \in \mathbb{R}^n$ is set during a transition from mode q to mode q'.

Definition 2: **(The dynamics of a Hybrid Automaton)**
As a hybrid system with explicitly shown modes, the continuous behavior in the hybrid automaton is modeled by a flow map $\dot{x} = f_q(x)$, while the discrete behavior is modeled by a jump map $\phi_q(x)$ (Cai et al., 2007). The conditions that permit flows and/or jumps are given by the flow set C and the jump set D, respectively, subsets of the state space. The dynamics of a hybrid automaton is given by

$$\mathcal{H} : \left\{ \begin{array}{ll} \dot{x} = f_q(x) & x \in C_q \\ \begin{bmatrix} x^+ \\ q^+ \end{bmatrix} \in \phi_q(x) & x \in D_q \end{array} \right\} \tag{1}$$

where

$$D_q = \bigcup_{e=(q,q') \in E} G(e); \qquad C_q = I_q; \tag{2}$$

$$\phi_q(x) = \bigcup_{e=(q,q'); x \in G(e)} \begin{bmatrix} R(e,x) \\ q' \end{bmatrix}; \tag{3}$$

$$C = \bigcup_{q \in Q} (C_q \times \{q\}); \quad D = \bigcup_{q \in Q} (D_q \times \{q\}) \tag{4}$$

The discrete transitions between modes are always guarded by zero-crossings of the guard functions, and continuous modes are always defined by a Boolean expression over discrete variables, which are piecewise constant in continuous time, this is to make sure that a mode change can only happen on discrete transitions. In general, there are three natural choices for the semantics of a zero-crossing $up(z)$(Schrammel, 2012):

- "At-zero" : $z(x_{k-1}, t_{k-1}) \leq 0 \wedge z(x_k, t_k) \geq 0$
- "Contact" : $z(x_{k-1}, t_{k-1}) < 0 \wedge z(x_k, t_k) \geq 0$
- "Crossing" : $z(x_{k-1}, t_{k-1}) \leq 0 \wedge z(x_k, t_k) > 0$

Based on non-standard analysis, by the continuity of the event function z in the "Crossing" semantics we can deduce that $z(t) = 0$ is valid at the zero-crossing point in standard semantics: by standardizing $z(t) \leq 0 \wedge z(t + \partial) > 0$ we get $st(z(t)) = st(z(t + \partial)) = 0$, where ∂ is a non-standard infinitesimal (Benveniste et al., 2012). This gives an unambiguous meaning to hybrid systems even if they contain chattering behavior. In order to allow chattering in the standard semantics, the trajectories are allowed to actually go above zero, up to a constant $\varepsilon > 0$.

Definition 3: **(Lie derivatives)**
Assume the flow map f_q is analytic in its second argument, the *Lie derivatives* $\mathcal{L}_{f_q}^k g_q : \mathbb{R}^n \to \mathbb{R}^n$ of a function

DOI 10.3384/ecp15119175

g_q, also analytic in its second argument, along f_q, for $k > 0$, is defined by:

$$\mathcal{L}_{f_q}^{k} g_q(x(t)) = \left(\frac{\partial \mathcal{L}_{f_q}^{k-1} g_q(x(t))}{\partial x(t)} \right) \cdot f_q(x(t)) \tag{5}$$

with

$$\mathcal{L}_{f_q}^{0} g_q(x(t)) = g_q(x(t)) \tag{6}$$

Definition 4: **(Pointwise relative degree)**
We define the relative degree $n_q(x) : \mathbb{R}^n \to \mathbb{N}$ by:

$$n_q(x) = k \; if \bigwedge_{j<k} \mathcal{L}_{f_q}^{j} g_q(x) = 0 \wedge \mathcal{L}_{f_q}^{k} g_q(x) \neq 0 \tag{7}$$

3 The Chattering Behavior

Physically, chattering behavior occurs if equal thresholds for the transition conditions of different modes are given and the system starts to oscillate around them. A specific issue is the existence of multiple sliding modes due to intersecting switching manifolds, that is, the chattering occurs on switching manifolds of different dimension, roughly speaking, the chattering set may belong to many $\mathbb{R}^{(n-r)}$ switching manifolds of the same system, where $r \in \{1, 2, ..., n\}$. To illustrate this particular case, we study, in the following, a mechanical stick-slip system with dry Coulomb friction.

3.1 Case Study 1:

The non-smooth system to be investigated (Figure 1), consists of three blocks of masses m, M_1, and M_2, where only the block of mass m is connected to a fixed support by a linear spring of stiffness k and is under the action of a sinusoidal external force u generated by an actuator P ($u = A \; sin(\omega \, t + \varphi)$). We denote x_m, x_{M_1}, and x_{M_2} to the position of the small mass m and the two inertial masses M_1 and M_2, respectively. We denote $\mathcal{F}_1$ to the tangential contact force on the frictional interface between the small mass m and the inertial mass M_1, and $\mathcal{F}_2$ to the tangential contact force on the frictional interface between the small mass m and the inertial mass M_2. The friction between the inertial mass M_2 and the ground is neglected. The origin of the displacements x_m, x_{M_1}, and x_{M_2} is taken where the spring is un-stretched. The system's state space representation is given by

$$f(x) : \left\{ \begin{array}{l} \dot{x}_m = v_m \\ \dot{v}_m = \frac{1}{m}(u - kx_m - \mathcal{F}_1 - \mathcal{F}_2) \\ \dot{x}_{M_1} = v_{M_1} \\ \dot{v}_{M_1} = \frac{1}{M_1}\mathcal{F}_1 \\ \dot{x}_{M_2} = v_{M_2} \\ \dot{v}_{M_2} = \frac{1}{M_2}\mathcal{F}_2 \end{array} \right\} \tag{8}$$

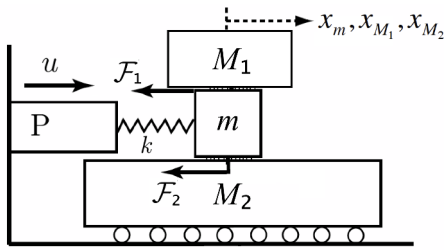

Figure 1. Schematic of the studied Stick-slip system.

where $x = [x_m \; v_m \; x_{M_1} \; v_{M_1} \; x_{M_2} \; v_{M_2}]^T$, and v_m, v_{M_1}, and v_{M_2} are the velocities of the small mass m and the inertial masses M_1 and M_2, respectively. In modeling friction-induced vibration and noise problems, friction force is often treated phenomenologically, as a function of relative velocity between surfaces.

$$\mathcal{F}_1 = \left\{ \begin{array}{l} -F_{c_1} \;\; for \;\; v_{r_1}(t) < 0 \\ \;\; F_{c_1} \;\; for \;\; v_{r_1}(t) > 0 \end{array} \right\} \tag{9}$$

$$\mathcal{F}_2 = \left\{ \begin{array}{l} -F_{c_2} \;\; for \;\; v_{r_2}(t) < 0 \\ \;\; F_{c_2} \;\; for \;\; v_{r_2}(t) > 0 \end{array} \right\} \tag{10}$$

where F_{c_1}, F_{c_2} are the levels of the Coulomb friction, $v_{r_1} = v_m - v_{M_1}$ is the relative velocity related to the masses m and M_1, and $v_{r_2} = v_m - v_{M_2}$ is the relative velocity related to the masses m and M_2. In the physical system, for the frictional interface between the small mass m and the inertial mass M_1, as long as the force acting at the interface (call it ρ_1) does not exceed the Coulomb friction level F_{c_1}, the two masses m and M_1 move together with $v_{r_1} = 0$. As soon as ρ_1 exceeds the Coulomb friction level, one mass slips over the other with $v_{r_1} \neq 0$. The slip is said to be positive ($Slip_1^+$) with a friction force $\mathcal{F}_1 = +F_{c_1}$ if $v_m > v_{M_1}$. The slip motion is said to be negative ($Slip_1^-$) with a friction force $\mathcal{F} = -F_{c_1}$ if $v_{M_1} > v_m$. The same applies for the interface between the masses m and M_2.
Obviously, we have a hybrid system with four explicitly shown modes $Q = \{q_1, q_2, q_3, q_4\}$, where the four modes $q_1 = slip_1^+ slip_2^+$, $q_2 = slip_1^- slip_2^+$, $q_3 = slip_1^- slip_2^-$, and $q_4 = slip_1^+ slip_2^-$ are distinguished by negative and positive relative velocities v_{r_1} and v_{r_2}. The hybrid automaton of this system is given, in the form (2), by

$$\mathcal{H} : \left\{ \begin{array}{l} \dot{x} \;\; = f_q(x) \;\; x \in C_q \\ \begin{bmatrix} x^+ \\ q^+ \end{bmatrix} \in \phi_q(x) \;\; x \in D_q \end{array} \right\} \tag{11}$$

$$f_1(x) : \left\{ \begin{array}{l} \dot{x}_m = v_m \\ \dot{v}_m = \frac{1}{m}(u - kx_m(t) - F_{c_1} - F_{c_2}) \\ \dot{x}_{M_1} = v_{M_1} \\ \dot{v}_{M_1} = \frac{1}{M_1}F_{c_1} \\ \dot{x}_{M_2} = v_{M_2} \\ \dot{v}_{M_2} = \frac{1}{M_2}F_{c_2} \end{array} \right\} \tag{12}$$

$$f_2(x): \left\{ \begin{array}{l} \dot{x}_m = v_m \\ \dot{v}_m = \frac{1}{m}(u - kx_m(t) + F_{c_1} - F_{c_2}) \\ \dot{x}_{M_1} = v_{M_1} \\ \dot{v}_{M_1} = \frac{-1}{M_1} F_{c_1} \\ \dot{x}_{M_2} = v_{M_2} \\ \dot{v}_{M_2} = \frac{1}{M_2} F_{c_2} \end{array} \right\} \tag{13}$$

$$f_3(x): \left\{ \begin{array}{l} \dot{x}_m = v_m \\ \dot{v}_m = \frac{1}{m}(u - kx_m(t) + F_{c_1} + F_{c_2}) \\ \dot{x}_{M_1} = v_{M_1} \\ \dot{v}_{M_1} = \frac{-1}{M_1} F_{c_1} \\ \dot{x}_{M_2} = v_{M_2} \\ \dot{v}_{M_2} = \frac{-1}{M_2} F_{c_2} \end{array} \right\} \tag{14}$$

$$f_4(x): \left\{ \begin{array}{l} \dot{x}_m = v_m \\ \dot{v}_m = \frac{1}{m}(u - kx_m(t) - F_{c_1} + F_{c_2}) \\ \dot{x}_{M_1} = v_{M_1} \\ \dot{v}_{M_1} = \frac{1}{M_1} F_{c_1} \\ \dot{x}_{M_2} = v_{M_2} \\ \dot{v}_{M_2} = \frac{-1}{M_2} F_{c_2} \end{array} \right\} \tag{15}$$

$$\phi_1(x) = \left\{ \begin{array}{ll} (x, q_2) & if\ v_{r_1} = 0 \wedge v_{r_2} \geq 0 \\ (x, q_4) & if\ v_{r_1} \geq 0 \wedge v_{r_2} = 0 \end{array} \right\} \tag{16}$$

$$\phi_2(x) = \left\{ \begin{array}{ll} (x, q_1) & if\ v_{r_1} = 0 \wedge v_{r_2} \geq 0 \\ (x, q_3) & if\ v_{r_1} \leq 0 \wedge v_{r_2} = 0 \end{array} \right\} \tag{17}$$

$$\phi_3(x) = \left\{ \begin{array}{ll} (x, q_2) & if\ v_{r_1} \leq 0 \wedge v_{r_2} = 0 \\ (x, q_4) & if\ v_{r_1} = 0 \wedge v_{r_2} \leq 0 \end{array} \right\} \tag{18}$$

$$\phi_4(x) = \left\{ \begin{array}{ll} (x, q_1) & if\ v_{r_1} \geq 0 \wedge v_{r_2} = 0 \\ (x, q_3) & if\ v_{r_1} = 0 \wedge v_{r_2} \leq 0 \end{array} \right\} \tag{19}$$

$$\begin{aligned} D_{q_1} &= G(q_1, q_2) \cup G(q_1, q_4) \qquad (20) \\ &= \{(v_{r_1} = 0 \wedge v_{r_2} \geq 0) \cup (v_{r_1} \geq 0 \wedge v_{r_2} = 0)\} \\ D_{q_2} &= G(q_2, q_1) \cup G(q_2, q_3) \qquad (21) \\ &= \{(v_{r_1} = 0 \wedge v_{r_2} \geq 0) \cup (v_{r_1} \leq 0 \wedge v_{r_2} = 0)\} \\ D_{q_3} &= G(q_3, q_2) \cup G(q_3, q_4) \qquad (22) \\ &= \{(v_{r_1} \leq 0 \wedge v_{r_2} = 0) \cup (v_{r_1} = 0 \wedge v_{r_2} \leq 0)\} \\ D_{q_4} &= G(q_4, q_1) \cup G(q_4, q_3) \qquad (23) \\ &= \{(v_{r_1} \geq 0 \wedge v_{r_2} = 0) \cup (v_{r_1} = 0 \wedge v_{r_2} \leq 0)\} \end{aligned}$$

Clearly, the system is discontinuous on two hyper switching manifolds Γ_a and Γ_b characterized as zero sets of the switching functions $\gamma_a(x)$ and $\gamma_b(x)$, respectively:

$$\Gamma_a = \{x \in \mathbb{R}^6 : \gamma_a(x) \models v_{r_1}(t) = 0\} \tag{24}$$

$$\Gamma_b = \{x \in \mathbb{R}^6 : \gamma_b(x) \models v_{r_2}(t) = 0\} \tag{25}$$

We will assume that $\frac{\partial \gamma_a(x)}{\partial x} \neq 0$ for all $x \in \Gamma_a$ and $\frac{\partial \gamma_b(x)}{\partial x} \neq 0$ for all $x \in \Gamma_b$ so that the normal units $\perp_a(x)$ and $\perp_b(x)$ orthogonal to the tangent planes $T_x(\Gamma_a)$ and $T_x(\Gamma_b)$, respectively, are well defined (Filippov, 1988). Furthermore, we assume that $\perp_a(x)$ and $\perp_b(x)$ are linearly independent for all $x \in \Gamma_a \cap \Gamma_b$. In the neighborhood of the intersection $\Delta = \Gamma_a \cap \Gamma_b$ (Figure 2), for the continuous time variables v_m, v_{M_1}, v_{M_2}, the $\mathbb{R}^3$ phase space consists of four open regions (the flow sets) C_i, for $i = 1,2,3,4$, with the flow map vector fields $f_1(x)$, $f_2(x)$, $f_3(x)$, and $f_4(x)$. The curve Δ is a $\mathbb{R}^{(n-2)}$ switching manifold results from the intersection of two transversally intersected $\mathbb{R}^{(n-1)}$ manifolds and is given by $\Delta = \Gamma_a \cap \Gamma_b = \{x \in \mathbb{R}^n : v_{r_1} = 0 \wedge v_{r_2} = 0\}$. Clearly, the curve Δ belongs to the boundary of each one of discrete states q_1, q_2, q_3, and q_4. Furthermore, each two adjacent regions are separated by a hyper switching manifold defined by opposed zero crossings of the same switching function. Let Γ be the entire discontinuity region in the phase space defined as the union of the two hyper switching manifolds Γ_a and Γ_b: $\Gamma = \Gamma_a \cup \Gamma_b$. A switching between the four different flow map's vector fields f_1, f_2, f_3, and f_4 takes place in the neighborhood of the intersection Δ. A trajectory that crosses Γ transversally will switch instantaneously between the vector fields f_q without any specific form of flow map vector on Γ. The only alternative is that a trajectory exhibits an attractive chattering on Γ, which yields an attractive chattering: i) between q_1 and q_2 on $\Gamma_{a_1} \in \mathbb{R}^{(n-1)}$, ii) between q_3 and q_4 on $\Gamma_{a_2} \in \mathbb{R}^{(n-1)}$, iii) between q_1 and q_4 on $\Gamma_{b_1} \in \mathbb{R}^{(n-1)}$, iv) between q_2 and q_3 on $\Gamma_{b_2} \in \mathbb{R}^{(n-1)}$, v) as well as between the four discrete states q_1, q_2, q_3, and q_4 on $\Delta \in \mathbb{R}^{(n-2)}$. On the intersection Δ, an infinite number of discrete transitions between the four modes is expected as long as for all $q \in Q$ the gradient of the continuous-time behavior according to the flow map's vector field f_q is directed into the intersection Δ, that is, in the neighborhood of the intersection the gradients direct behavior towards Δ so that upon each entering to a new mode an infinitesimal step causes another mode change. When simulating this system, in general, such behavior breaks down the numerical integration of the dynamics, as it does not progress in time, but chatters between modes.

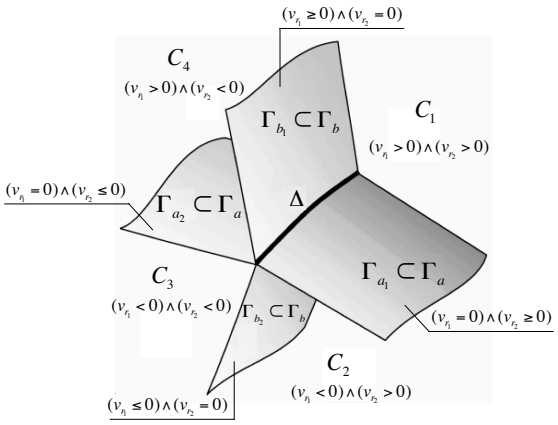

Figure 2. The switching intersection set in the $\mathbb{R}^3$-dimensional phase space of the studied system.

3.2 Chattering in The Neighborhood of a Switching Intersection:

We consider a hybrid automaton $\mathcal{H}$ with a finite set of discrete states $q \in Q$ with transverse invariants (Morris, 2009) where the state space is split into different regions (flow sets $C_q \in \mathbb{R}^n$) by the intersection of p transversally intersected $\mathbb{R}^{n-1}$ switching manifolds Γ_j defined as the zeros of a set of scalar functions $\gamma_j(x)$ for $j = 1,2,...,p$,

$$\Gamma_j = \{x \in \mathbb{R}^n : \ \gamma_j(x) = 0 \ ; \quad j = 1,2,...,p\} \tag{26}$$

The zero crossing in opposite directions defines the switching between two adjacent flow sets. All switching functions γ_j are assumed to be analytic in their second arguments so the normal unit vector $\perp_j$ for each one of the intersected switching manifolds Γ_j is well defined. Moreover, the normal unit vectors are linearly independent for all the $\mathbb{R}^{(n-r)}$ intersections where $r \in \{2,3,...,n\}$. The system phase space $C \subseteq \mathbb{R}^n$ is partitioned into 2^p open convex regions (sub-domains) $C_q \in \mathbb{R}^n$, $q = 1,...2^p$, and p switching manifold $\gamma_j(x) \in \mathbb{R}^{n-1}$, $j = 1,2,...,p$. In the convex flow sets C_q, the solution trajectory flow is governed by different vector fields $f_q(x(t))$. Furthermore, it is assumed that the flow maps f_q are smooth in the state x for any open flow set adjacent to the flow set C_q and all f_q can be associated to the intersection.
In general, the disjoint 2^p regions flow sets can be characterized in a systematic way by defining a sign matrix Ψ of size $(p, 2^p)$ as following:
Let $W^{(k)} = (W_i)_{1,2^k}$ be an 1×2^k vector of values $W_i = 1$, $\forall i$, with $k = 1,...,p-1$.

1. The first row vector of the matrix Ψ: $V_1 = \Psi(1,:)$ consists of 2^{p-1} pairs of $\left(-W^{(1)}(1,1), W^{(1)}(1,2)\right)$.

$$\Psi^{(1)} = \{-W^{(1)}(1,1), W^{(1)}(1,2)\}_{2^{p-1}} \tag{27}$$

2. The second row vector $V_2 = \Psi(2,:)$ consists of 2^{p-2} pairs of $(-W^{(1)}, W^{(1)})$.

$$\Psi^{(2)} = \{-W^{(1)}, W^{(1)}\}_{2^{p-2}} \tag{28}$$

3. The jth row vector $V_j = \Psi(j,:)$ consists of 2^{p-j} pairs of $(-W^{(j-1)}, W^{(j-1)})$ for $j = 3,...,p$.

$$\Psi^{(j)} = \{-W^{(j-1)}, W^{(j-1)}\}_{2^{p-j}} \tag{29}$$

Each column vector defines the signs of the switching functions $\gamma_j(x)$ for a given flow set C_q. We use the multi-valued function $\alpha_j(x)$ such that the convex set is given for all $\Gamma_j|_{j=1,2,...,p}$ and $C_i|_{i=1,2,...,2^p}$ by:

$$\dot{x} \in \sum_{i=1}^{2^p} \left((\prod_{j=1}^{p} \frac{1 + 2\Psi_{j,i} \cdot \alpha_j(x) - \Psi_{j,i}}{2}) \cdot f_i(x) \right) \tag{30}$$

where

$$\alpha_j(x) = \left\{ \begin{array}{cc} 1 & for \ \gamma_j(x) > 0 \\ [0,1] & for \ \gamma_j(x) = 0 \\ 0 & for \ \gamma_j(x) < 0 \end{array} \right\} \tag{31}$$

$$\sum_{i=1}^{2^p} \left(\prod_{j=1}^{p} \frac{1 + 2\Psi_{j,i} \cdot \alpha_j - \Psi_{j,i}}{2} \right) = 1 \tag{32}$$

Equation (31) yields in

$$\dot{x} \in (1 - \alpha_j) \cdot \sum_{i=1}^{2^p} (R_1 \cdot f_i(x)) + \alpha_j \cdot \sum_{i=1}^{2^p} (R_2 \cdot f_i(x)) \tag{33}$$

$$R_1 = \prod_{k=1;k \neq j;\Psi_{k,i}=-1}^{p} \left(\frac{1 + 2\Psi_{k,i} \cdot \alpha_k - \Psi_{k,i}}{2} \right) \tag{34}$$

$$R_2 = \prod_{k=1;k \neq j;\Psi_{k,i}=1}^{p} \left(\frac{1 + 2\Psi_{k,i} \cdot \alpha_k - \Psi_{k,i}}{2} \right) \tag{35}$$

We then define a matrix F of the normal projections $f_i^{\perp_j}(x)$ for $j = 1,2,...,p$ and $i = 1,2,...,2^p$ as

$$F = \left\{ \begin{array}{cccc} f_1^{\perp_1}(x) & f_1^{\perp_2}(x) & \cdots & f_1^{\perp_p}(x) \\ f_2^{\perp_1}(x) & f_2^{\perp_2}(x) & \cdots & f_2^{\perp_p}(x) \\ \vdots & \vdots & \ddots & \vdots \\ \vdots & \vdots & \ddots & \vdots \\ f_{2^p}^{\perp_1}(x) & f_{2^p}^{\perp_2}(x) & \cdots & f_{2^p}^{\perp_p}(x) \end{array} \right\} \tag{36}$$

where

$$f_i^{\perp_j}(x) = \mathcal{L}_{f_i}\gamma_j(x) = \left(\frac{\partial \gamma_j(x)}{\partial x} \right)^T \cdot f_i(x) \tag{37}$$

In agreement with the sign matrix Ψ, the attractive chattering on any $\mathbb{R}^{(n-r)}$ switching manifold for $r = 2,3,...,n$ can be easily observed by checking the signs of the matrices F and Ψ.

Lemma 1:
The sufficient condition for having an attractive chattering on any switching intersection in the system's state space requires a nodal attractivity towards the intersection itself, for all the flow maps f_i in the $\mathbb{R}^n$ regions C_i associated to this intersection. That is, the following constraint should be satisfied

$$\forall i, j : \ sgn(f_i^{\perp_j}(x)) = -sgn(\Psi_{j,i}) \tag{38}$$

To keep the solution trajectory in a sliding motion on the intersection as long as the attractive chattering condition is satisfied we impose

$$\forall j = 1,2,...p :$$

$$\sum_{i=1}^{2^p} (\prod_{j=1}^{p} \frac{1 + 2\Psi_{j,i} \cdot \alpha_j - \Psi_{j,i}}{2}) \cdot f_i^{\perp_j}(x) = 0 \tag{39}$$

so that

$$\alpha_j = \frac{W_1}{W_1 - W_2} \tag{40}$$

$$W_1 = \sum_{i=1}^{2^p} \Big(\prod_{k=1;k\neq j;\Psi_{k,i}=-1}^{p} \frac{1+2\Psi_{k,i}\cdot\alpha_k - \Psi_{k,i}}{2} \Big) \cdot f_i^{\perp j} \tag{41}$$

$$W_2 = \sum_{i=1}^{2^p} \Big(\prod_{k=1;k\neq j;\Psi_{k,i}=1}^{p} \frac{1+2\Psi_{k,i}\cdot\alpha_k - \Psi_{k,i}}{2} \Big) \cdot f_i^{\perp j} \tag{42}$$

For all $\alpha_k \in (0,1)$, the product term in (42) (respectively (43)) takes always a value in (0,1) since it is always a product of $(1-\alpha_k)$ (respectively α_k). It holds always that $W_1 > 0 \wedge W_2 < 0$ as long as an attractive chattering takes place at $x \in \left(\bigcup_{j=1}^{p} \Gamma_j\right) \cap C$, where C is the entire flow set in the system phase space.

This gives us a hypercube convex hull of sign coordiantes (± 1, ± 1, $\cdots$, ± 1) with an edge of length 2 and $\mathbb{R}^n$ volume 2^p. Therefore, a solution to the fixed point nonlinear problem (40) exists. However, the uniqueness of the solution is no guaranteed. To deal with non-uniqueness on the intersection−on which the attractive chattering occurs−we propose to give an equivalent to the product term in (40) so that the sliding parameters are given in term of a rational function of coefficients κ_i:

$$\prod_{j=1}^{p} \frac{1+2\Psi_{j,i}\cdot\alpha_j - \Psi_{j,i}}{2} = \frac{\kappa_i}{\sum_{k=1}^{2^p}\kappa_k} \tag{43}$$

where

$$\kappa_i = \frac{\left(\prod_{l=1;l\neq i}^{2^p}(\Omega_l)\right)^{\frac{1}{2^p-1}}}{\left(\prod_{l=1;l\neq i}^{2^p}(\Omega_l)\right)^{\frac{1}{2^p-1}} - (\Omega_i)} \tag{44}$$

$$\Omega_i = [(b_i)_1\ (b_i)_2\ \cdots\ (b_i)_p] \cdot \begin{bmatrix} \mathcal{L}_{f_i}\gamma_1(x) \\ \mathcal{L}_{f_i}\gamma_2(x) \\ \vdots \\ \mathcal{L}_{f_i}\gamma_p(x) \end{bmatrix} \tag{45}$$

$$\Omega_l = [(b_l)_1\ (b_l)_2\ \cdots\ (b_l)_p] \cdot \begin{bmatrix} \mathcal{L}_{f_l}\gamma_1(x) \\ \mathcal{L}_{f_l}\gamma_2(x) \\ \vdots \\ \mathcal{L}_{f_l}\gamma_p(x) \end{bmatrix} \tag{46}$$

The vectors b_n for $n = i,l$ are given as sign permutations of coordinates $[\pm 1, \pm 1, \cdots, \pm 1]^T$ under the constraint:

$$sgn(b_n)_j = \left\{ \begin{array}{c} sgn(\mathcal{L}_{f_n}\gamma_j(x)) \ \ for\ \ n=1 \\ -sgn(\mathcal{L}_{f_n}\gamma_j(x)) \ \ for\ \ n=2,3,...,2^p \end{array} \right\} \tag{47}$$

where $j = 1,2,...,p$ and p is the number of the intersected $\mathbb{R}^{(n-1)}$ switching manifolds. This gives always $\Omega_1 > 0$ and $\Omega_n < 0$ for all $n \in \{2,3,..,2^p\}$ which is exactly what we want. Another advantage of using the signs constraint in (48) is that $\kappa_j = 0$ for all $j \neq i$ when $\kappa_i = 1$ for a given index $i \in \{1,2,...,2^p\}$, this allows us to detect when a switching regime of different dimension has been reached by the solution trajectory, and then, to select the appropriate vector fields on this regime. Moreover, the parameter κ_i takes always a value $0 \leq \kappa_i \leq 1$ for $i = 1,2,...,2^p$, yields in $\sum_{i=1}^{2^p}\left(\frac{\kappa_i}{\sum_{k=1}^{2^p}\kappa_k}\right) = 1$, which is consistent with the approach of Filippov differential inclusion.

Case Study 1 Revisited:
With $A = u - kx_m$, the Lie derivatives of the switching functions $\gamma_a(x)$ and $\gamma_b(x)$ along the flow map vector fields f_1, f_2, f_3, and f_4 are given by

$$f_1^{\perp a}(x) = \frac{1}{m}\cdot\left(A - (\frac{m+M_1}{M_1})\cdot F_{c_1} - F_{c_2}\right) \tag{48}$$

$$f_1^{\perp b}(x) = \frac{1}{m}\cdot\left(A - F_{c_1} - (\frac{m+M_2}{M_2})\cdot F_{c_2}\right) \tag{49}$$

$$f_2^{\perp a}(x) = \frac{1}{m}\cdot\left(A + (\frac{m+M_1}{M_1})\cdot F_{c_1} - F_{c_2}\right) \tag{50}$$

$$f_2^{\perp b}(x) = \frac{1}{m}\cdot\left(A + F_{c_1} - (\frac{m+M_2}{M_2})\cdot F_{c_2}\right) \tag{51}$$

$$f_3^{\perp a}(x) = \frac{1}{m}\cdot\left(A + (\frac{m+M_1}{M_1})\cdot F_{c_1} + F_{c_2}\right) \tag{52}$$

$$f_3^{\perp b}(x) = \frac{1}{m}\cdot\left(A + F_{c_1} + (\frac{m+M_2}{M_2})\cdot F_{c_2}\right) \tag{53}$$

$$f_4^{\perp a}(x) = \frac{1}{m}\cdot\left(A - (\frac{m+M_1}{M_1})\cdot F_{c_1} + F_{c_2}\right) \tag{54}$$

$$f_4^{\perp b}(x) = \frac{1}{m}\cdot\left(A - F_{c_1} + (\frac{m+M_2}{M_2})\cdot F_{c_2}\right) \tag{55}$$

. We distinguish between the following cases:

- An infinitely fast back and forth switching between the discrete states q_1 and q_2 occurs on Γ_{a_1} if and only if $f_1^{\perp a}(x) < 0 \wedge f_2^{\perp a}(x) > 0$. This happens when $|(u - kx_m - F_{c_2})| < (\frac{m+M_1}{M_1})\cdot F_{c_1}$. The resulting sliding vector field $f_{s_{a_1}}$ is:

$$f_{s_{a_1}} = \left\{ \begin{array}{c} v_m \\ \frac{1}{m+M_1}(u - kx_m - F_{c_2}) \\ v_{M_1} \\ \frac{1}{m+M_1}(u - kx_m - F_{c_2}) \\ v_{M_2} \\ \frac{1}{M_2}F_{c_2} \end{array} \right\} \tag{56}$$

- An infinitely fast back and forth switching between the discrete states q_3 and q_4 occurs on Γ_{a_2} if and only if $f_4^{\perp a}(x) < 0 \wedge f_3^{\perp a}(x) > 0$. This happens when

$|(u-kx_m+F_{c_2})| < (\frac{m+M_1}{M_1})\cdot F_{c_1}$. The resulting sliding vector field $f_{s_{a_2}}$ is:

$$f_{s_{a_2}} = \left\{ \begin{array}{l} v_m \\ \frac{1}{m+M_1}(u-kx_m+F_{c_2}) \\ v_{M_1} \\ \frac{1}{m+M_1}(u-kx_m+F_{c_2}) \\ v_{M_2} \\ \frac{-1}{M_2}F_{c_2} \end{array} \right\} \tag{57}$$

- An infinitely fast back and forth switching between the discrete states q_1 and q_4 occurs on Γ_{b_1} if and only if $f_1^{\perp b}(x) < 0 \wedge f_4^{\perp b}(x) > 0$. This happens when $|(u-kx_m-F_{c_1})| < (\frac{m+M_2}{M_2})\cdot F_{c_2}$. The resulting sliding vector field $f_{s_{b_1}}$ is:

$$f_{s_{b_1}} = \left\{ \begin{array}{l} v_m \\ \frac{1}{m+M_2}(u-kx_m-F_{c_1}) \\ v_{M_1} \\ \frac{1}{M_1}F_{c_1} \\ v_{M_2} \\ \frac{1}{m+M_2}(u-kx_m-F_{c_1}) \end{array} \right\} \tag{58}$$

- An infinitely fast back and forth switching between the discrete states q_2 and q_3 occurs on Γ_{b_2} if and only if $f_2^{\perp b}(x) < 0 \wedge f_3^{\perp b}(x) > 0$. This happens when $|(u-kx_m+F_{c_1})| < (\frac{m+M_2}{M_2})\cdot F_{c_2}$. The resulting sliding vector field $f_{s_{b_2}}$ is:

$$f_{s_{b_2}} = \left\{ \begin{array}{l} v_m \\ \frac{1}{m+M_2}(u-kx_m+F_{c_1}) \\ v_{M_1} \\ \frac{-1}{M_1}F_{c_1} \\ v_{M_2} \\ \frac{1}{m+M_2}(u-kx_m+F_{c_1}) \end{array} \right\} \tag{59}$$

- An infinitely fast switching between q_1, q_2, q_3, and q_4 takes place on the intersection Δ if and only if the following four conditions are satisfied

  1. $(f_1^{\perp\Gamma_a} < 0) \wedge (f_2^{\perp\Gamma_a} > 0)$ which happens when $|(A-F_{c_2})| < (\frac{m+M_1}{M_1})\cdot F_{c_1}$.
  2. $(f_1^{\perp\Gamma_b} < 0) \wedge (f_4^{\perp\Gamma_b} > 0)$ which happens when $|(A-F_{c_1})| < (\frac{m+M_2}{M_2})\cdot F_{c_2}$.
  3. $(f_2^{\perp\Gamma_b} < 0) \wedge (f_3^{\perp\Gamma_b} > 0)$ which happens when $|(A+F_{c_1})| < (\frac{m+M_2}{M_2})\cdot F_{c_2}$.
  4. $(f_4^{\perp\Gamma_a} < 0) \wedge (f_3^{\perp\Gamma_a} > 0)$ which happens when $|(A+F_{c_2})| < (\frac{m+M_1}{M_1})\cdot F_{c_1}$.

The resulting sliding vector field f_{s_Δ} is:

$$f_{s_\Delta} = \left\{ \begin{array}{l} v_m \\ \frac{1}{m+M_1+M_2}(u-kx_m) \\ v_{M_1} \\ \frac{1}{m+M_1+M_2}(u-kx_m) \\ v_{M_2} \\ \frac{1}{m+M_1+M_2}(u-kx_m) \end{array} \right\} \tag{60}$$

4 Numerical Approach:

The algorithm has to detect: (i) when a switching manifold of different dimension is reached, and (ii) whether the trajectory stays on or leaves the switching manifold. This has to be decided depending on the gradients of the continuous time behavior in the neighborhood of the current state. Let $\Gamma = \bigcup_{j=1}^{p}\Gamma_j$ be the entire discontinuity region. The algorithm has to perform the following tasks: (1) Robust integration outside the entire discontinuity region Γ; (2) Accurate detection and location of the switch points x_m when the solution trajectory reaches Γ, this includes switching intersections for lower dimensions; (3) Check at $x_m \in \Gamma$ for the existence of a regular switching (transversality) as well as for the existence of an attractive chattering behavior (sliding motion); (4) Integration with a sliding mode on Γ; (5) Decision of whether or not we should leave the sliding region. We would like to mention that our contribution is **independent** of using particular integration schemes. For discretizing the differential equations outside the discontinuity region Γ any explicit integration scheme can be used. In this work we have used the mid-point rule of explicit 2nd order Runge-Kutta integration scheme (Butcher, 2008; Cellier and Kofman, 2006; Munz et al., 2011). At the end of each integration step we check whether the discontinuity region Γ has been reached or not. We distinuiush the following cases:

1. If $\langle \gamma_j(x_i)\cdot\gamma_j(x_{i+1})\rangle > 0$ for all $j = 1,2,...,p$ where p is the number of the intersected $\mathbb{R}^{(n-1)}$ switching manifolds, then we continue integrating the system with the same flow map vector f_q.
2. If there exist $j \in \{1,2,...,p\}$ such that $\langle \gamma_j(x_i)\cdot\gamma_j(x_{i+1})\rangle < 0$, this indicates a zero crossing in the time interval $(t_i, t_i+\Delta t_i)$. In this case we have a continuous smooth switching function $\gamma_j(x_{i+1}(\sigma))$ taking opposed signs at $\sigma = 0$ and $\sigma = \Delta T_i$ and therefore there exist a zero at $\sigma_m \in (0,\Delta T_i)$ which defines the switch point $x_m = x_{i+1}(\sigma_m) \in \Gamma_j$.
3. The case in which we have $\langle \gamma_j(x_i)\cdot\gamma_j(x_{i+1})\rangle < 0 \wedge \gamma_j(\sigma_m) = 0$ for all $j = 1,2,...,k$ where $k \le p$ and $\sigma_m \in (0,\Delta T_i)$ indicates that the solution trajectory has reached the intersection of $k \le p$ of transvrsally intersected $\mathbb{R}^{(n-1)}$ hyper switching manifolds Γ_j.

In the last two cases, secant approach (Allen and Isaacson, 1998; Kaw and Kalu, 2008) is employed to find the root

σ_m of the switching function $\gamma_j(\sigma) = \gamma(x_{i+1}(\sigma))$. Once the switch point x_m has been located, the algorithm checks whether the switch point x_m is a transversality point (leads to cross Γ) or a chattering equilibrium (leads to slide on Γ) by checking the sign of the two matrices Ψ and F (Lemma 1). The proposed convexification (Equation 40, 44-48) is used to approximate the system dynamics when sliding on Γ. For the integration during the sliding any implicit integration scheme can be used. In this work we have used the midpoint rule of implicit Bathe time integration scheme (Bathe and Noh, 2012). To avoid any situation in which the intermediate stages values don't lie exactly on the sliding surface we use a projection formulation for convex sets together with semi-smooth Newton methods to project back to the sliding region the approximated stage values $x_{i+\frac{1}{2}}$ and x_{i+1} at $t_i + \frac{\Delta t_i}{2}$ and $t_i + \Delta t_i$, respectively. The objective of the projection formulation is to stabilize the solution during the sliding on Γ. Consider a point x^* close to the hyper switching manifold Γ, each one integration step of the projected Bathe scheme on the sliding manifold Γ_s then is given as

1. $x^*_{i+\frac{1}{2}} = x_i + \frac{\Delta t_i}{4}\left(f_s(x_i) + f_s(x_{i+\frac{1}{2}})\right)$
2. $x_{i+\frac{1}{2}} = proj(x^*_{i+\frac{1}{2}})$
3. $x^*_{i+1} = -\frac{1}{3}x_i + \frac{4}{3}x_{i+\frac{1}{2}} + \frac{\Delta t_i}{3} f_s(x_{i+1})$
4. $x_{i+1} = proj(x^*_{i+1})$

The projection point $x \in \Gamma$ to x^*: $x = P(x^*)$ is given by the solution of the projection function:

$$P : \min_{x \in \Gamma_s} u(x) : \quad u(x) = \left(\frac{1}{2}(x^* - x)^T (x^* - x)\right) \tag{61}$$

where Γ_s is the sliding manifold. To find the projected value x we introduce a Lagrange multiplier λ and we need to find the root of the equation system

$$G(x,\lambda) = \begin{pmatrix} \frac{\partial u(x)}{\partial x} + \lambda \frac{\partial \gamma(x)}{\partial x} \\ \gamma(x) \end{pmatrix} \tag{62}$$

We use Newton iteration, by imposing the condition $G(x_{k+1}, \lambda_{k+1}) = 0$ and expand $G(x_{k+1}, \lambda_{k+1})$ in Taylor series neglecting the terms of order equal or greater than 2.

$$0 = G(x_k, \lambda_k) + \begin{pmatrix} x_{k+1} - x_k \\ \lambda_{k+1} - \lambda_k \end{pmatrix} \cdot G'(x_k, \lambda_k) \tag{63}$$

for $k \geq 0$ so that

$$G'(x_k, \lambda_k) \cdot \begin{pmatrix} x_{k+1} - x_k \\ \lambda_{k+1} - \lambda_k \end{pmatrix} = -G(x_k, \lambda_k) \tag{64}$$

$$G'(x,\lambda) = \begin{bmatrix} I + \lambda \frac{\partial}{\partial x}\left(\frac{\partial \gamma(x)}{\partial x}\right) & \frac{\partial \gamma(x)}{\partial x} \\ \left(\frac{\partial \gamma(x)}{\partial x}\right)^T & 0 \end{bmatrix} \tag{65}$$

At the end of each integration step from t_i to $t_i + \Delta t_i$ while we integrate with the sliding vector f_s, we keep checking whether we have to keep sliding on Γ_s or leaving it, by checking the value of κ_i in (45).

5 Simulation Results:

As shown in Figure 3, the system in Case Study 1 was simulated for $m = M_1 = M_2 = 1[kg]$, $k = 0.88[N \cdot m^{-1}]$, $F_{c_1} = 0.01996[N]$ $F_{c_2} = 0.062[N]$, and $x_0 = [0.8295\ 0.8491\ 0.3725\ 0.5932\ 0.8726\ 0.9335]^T$. The force u was simulated as a sine wave of frequency of $\omega = 0.073[rad/sec]$. The relative and absolute error tolerance used in the approximation were adjusted to $ATOL = RTOL = 10^{-8}$.

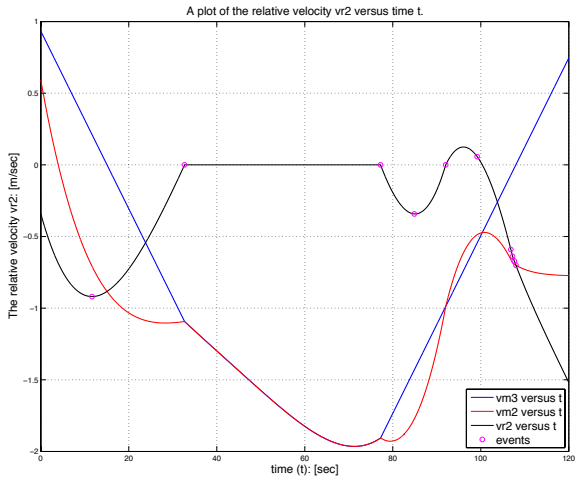

(a)

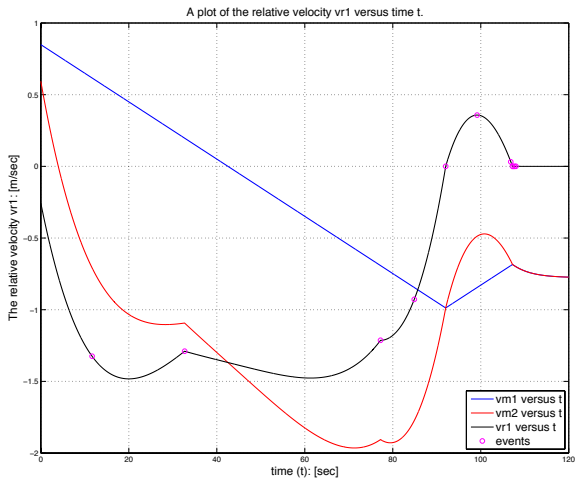

(b)

Figure 3. The sliding mode simulation of Example 2.4 with $m = M_1 = M_2 = 1[kg]$, $k = 0.88[N \cdot m^{-1}]$, $F_{c_1} = 0.01996[N]$ $F_{c_2} = 0.062[N]$, and $x_0 = [0.8295\ 0.8491\ 0.3725\ 0.5932\ 0.8726\ 0.9335]^T$. In (a): The time evolution of the relative velocity v_{r_2}. In (b): The time evolution of the velocities v_{r_1}.

The sliding bifurcations depend on the effect of the external force u and the level of Coulomb friction. We can observe that, at the beginning of the simulation, the

DOI 10.3384/ecp15119175

execution of the hybrid automaton starts in the discrete state $q_3 = Slip_1^- Slip_2^-$, the system starts in a slip phase for the two frictional interfaces in the system; since the effect of the external force applied tangentially on the interface is lower than the level of Coulomb friction. At the time instant $t = 32.69$ *sec*, two masses m and M_2 stick together and the solution trajectory start a sliding motion on the switching manifold Γ_{b_2} (see Figure 3 (a)) ensuring a chattering path avoidance between the discrete states $q_3 = Slip_1^- Slip_2^-$ and $q_2 = Slip_1^- Slip_2^+$. A smooth exit from the sliding motion on Γ_{b_2} into q_3 was detected at the time instant $t = 77.23$ *sec*. A regular switching (transversality) from the discrete state $q_3 = Slip_1^- Slip_2^-$ to the discrete state $q_1 = Slip_1^+ Slip_2^+$ at the intersection $\Delta = \Gamma_a \cap \Gamma_b$ was detected at $t = 92.04$ *sec*. At $t = 108$ *sec*, two masses m and M_1 stick together and the solution trajectory start a sliding motion on the switching manifold Γ_{a_2} ensuring a chattering path avoidance between the discrete states $q_4 = Slip_1^+ Slip_2^-$ and $q_3 = Slip_1^- Slip_2^-$. During a simulation time of 120 seconds, 5 mode switches have been recorded.

Case Study 2:
Consider a mechanical system as depicted in Figure 4. The system consists of three blocks of masses m_1, m_2, and m_3 on a moving belt with constant velocity v_d. The three blocks are connected along a line by two linear springs of stiffness k_{12} and k_{23}, and connected to a fix support by to linear springs of stiffness k_1, k_2, and k_3, respectively.

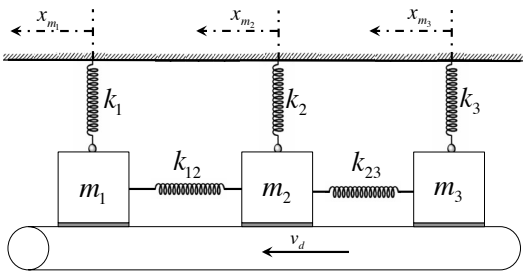

Figure 4. The schematic of the studied Mechanical stick-slip system with 3 blocks.

The equations of the system model in $\mathbb{R}^6$ are given by

$$f(x) : \left\{ \begin{array}{l} \dot{x}_{m_1}(t) = v_{m_1}(t) \\ \dot{v}_{m_1}(t) = \frac{1}{m_1}(u_1 - k_1 x_{m_1}(t) - \mathcal{F}_1) \\ \dot{x}_{m_2}(t) = v_{m_2}(t) \\ \dot{v}_{m_2}(t) = \frac{1}{m_2}(u_2 - k_2 x_{m_2}(t) - \mathcal{F}_2) \\ \dot{x}_{m_3}(t) = v_{m_3}(t) \\ \dot{v}_{m_3}(t) = \frac{1}{m_3}(u_3 - k_3 x_{m_3}(t) - \mathcal{F}_3) \end{array} \right\} \quad (66)$$

$$u_1 = k_{12}(x_{m_2} - x_{m_1}) + k_{13}(x_{m_3} - x_{m_1}) \quad (67)$$

$$u_2 = k_{12}(x_{m_1} - x_{m_2}) + k_{23}(x_{m_3} - x_{m_2}) \quad (68)$$

$$u_3 = k_{13}(x_{m_1} - x_{m_3}) + k_{23}(x_{m_2} - x_{m_3}) \quad (69)$$

We denote x_{m_1}, x_{m_2}, and x_{m_3} to the position of the masses m_1, m_2, and m_3 respectively, $\mathcal{F}_1$, $\mathcal{F}_2$, and $\mathcal{F}_3$ to the tangential contact force on the frictional interfaces between the moving belt and the three masses m_1, m_2, and m_3 respectively. The functional relationship between the friction force and the relative velocity on the three frictional interfaces between the moving belt and the blocks m_1, m_2, and m_3 is given by

$$\mathcal{F}_1 = \left\{ \begin{array}{l} F_{c_1} \ for \ v_{m_1} > v_d \\ -F_{c_1} \ for \ v_{m_1} < v_d \end{array} \right\} \quad (70)$$

$$\mathcal{F}_2 = \left\{ \begin{array}{l} F_{c_2} \ for \ v_{m_2} > v_d \\ -F_{c_2} \ for \ v_{m_2} < v_d \end{array} \right\} \quad (71)$$

$$\mathcal{F}_3 = \left\{ \begin{array}{l} F_{c_3} \ for \ v_{m_3} > v_d \\ -F_{c_3} \ for \ v_{m_3} < v_d \end{array} \right\} \quad (72)$$

where v_{m_1}, v_{m_2}, and v_{m_3} are the velocities of m_1,m_2, and m_3 respectively. F_{c_1}, F_{c_2}, and F_{c_3} are the levels of the coulomb friction. Physically, for each one of the three frictional interfaces in the system, as long as the force acting at the interface (call it ρ_j) does not exceed the Coulomb friction level F_{c_j}, the moving belt and the mass m_j move together with $v_{r_j} = 0$ where $j = 1,2,3$. As soon as ρ_j exceeds the Coulomb friction level, the mass m_j slips over the belt with $v_{r_j} \neq 0$. The slip is said to be positive ($Slip_j^+$) with a friction force $\mathcal{F}_j = +F_{c_j}$, i.e. the mass m_j slips on the belt, if $v_j > v_d$. The slip motion is said to be negative ($Slip_j^-$) with a friction force $\mathcal{F} = -F_{c_j}$, if $v_j < v_d$. Obviously the system is discontinuous on three hyper switching manifolds Γ_a, Γ_b, and Γ_c characterized as zero sets of the switching functions $\gamma_a(x)$, $\gamma_b(x)$, and $\gamma_c(x)$ respectively

$$\Gamma_a = \{x \in \mathbb{R}^n : \gamma_a(x) \models v_{m_1}(t) = v_d(t)\} \quad (73)$$

$$\Gamma_b = \{x \in \mathbb{R}^n : \gamma_b(x) \models v_{m_2}(t) = v_d(t)\} \quad (74)$$

$$\Gamma_c = \{x \in \mathbb{R}^n : \gamma_c(x) \models v_{m_3}(t) = v_d(t)\} \quad (75)$$

The system was simulated for the data set: $m_1 = m_2 = m_3 = 1[kg]$, $F_{c_1} = 0.14[N]$, $F_{c_2} = 0.13[N]$, $F_{c_3} = 0.12[N]$, $k_1 = k_2 = k_3 = k_{12} = k_{13} = k_{23} = 0.01[N \cdot m^{-1}]$, $v_d = 0.5m/sec$ and $x_0 = [4.7799\ 0.2797\ 4.0038\ 1.7144\ 1.2922\ 4.1263]^T$. The external force u was simulated as a sine wave of frequency of $\omega = 0.24[rad/sec]$. The relative and absolute error tolerance used in the approximation were adjusted to $ATOL = RTOL = 10^{-8}$.
The simulation results for simulation time adjusted to 100 seconds are shown in Figure 5. At the beginning of the simulation, the execution of the hybrid automaton starts in the discrete state $q_1 = Slip_1^+ Slip_2^+ Slip_3^+$ (i.e. the system starts in a slip phase), since the effect of the external force applied tangentially on the frictional interface is greater than the level of Coulomb friction, for the three frictional interfaces in the system. Both m_1 and m_2 stick with the moving belt in the time interval from $t = 74.84sec$ to $t = 89.07sec$ and the solution

trajectory start a sliding motion on the intersection $\Gamma_a \cap \Gamma_b = \{x \in \mathbb{R}^6 : v_{m_1} = v_{m_2} = v_d\}$. At the time instant $t = 76.69sec$ the solution passes through the intersection of the three transversally intersected switching manifolds $\Gamma_a \cap \Gamma_b \cap \Gamma_c = \{x \in \mathbb{R}^6 : v_{m_1} = v_{m_2} = v_{m_3} = v_d\}$ switching from a sliding on the intersection $\Gamma_a \cap \Gamma_b$ in the positive direction of the switching manifold Γ_c into sliding on the intersection $\Gamma_a \cap \Gamma_b$ in the negative direction of Γ_c providing a chattering bath avoidance between the flow sets associated to these intersections. During a simulation time of 100 seconds, 16 mode switches as well as 12 tangential crossings have been recorded.

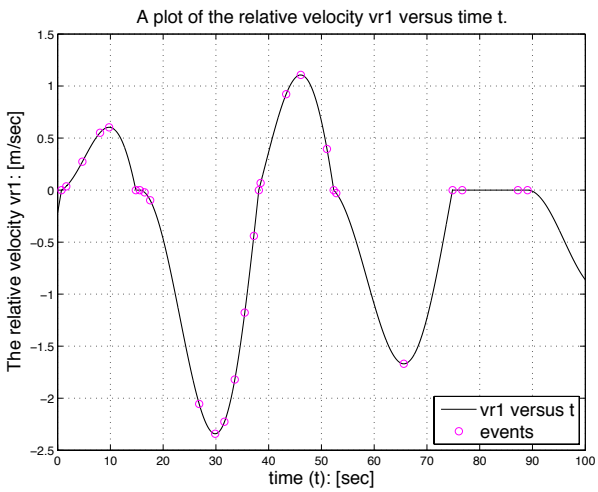

(a)

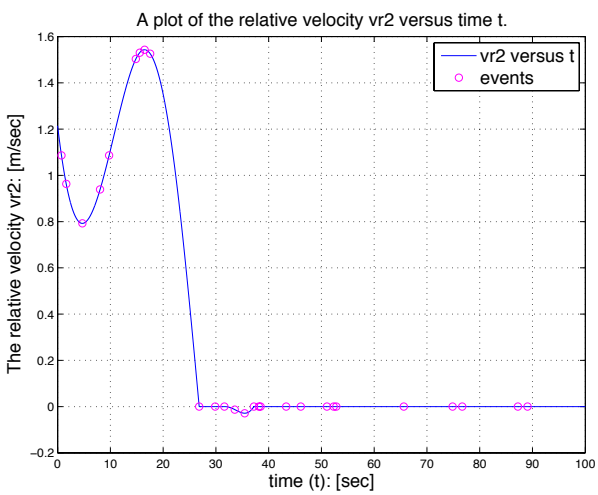

(b)

Figure 5. The sliding mode simulation of Case Study 2 with $m_1 = m_2 = m_3 = 1[kg]$, $k_1 = k_2 = k_3 = k_{12} = k_{13} = k_{23} = 0.01[N \cdot m^{-1}]$, $F_{c_1} = 0.14[N]$ $F_{c_2} = 0.13[N]$, $F_{c_3} = 0.12[N]$, $v_d = 0.5m/sec$, and $x_0 = [4.7799\ 0.2797\ 4.0038\ 1.7144\ 1.2922\ 4.1263]^T$. In (a): The time evolution of the relative velocity v_{r_1}. In (b): The time evolution of the relative velocity v_{r_2}.

6 Conclusions

In this paper we presented a new approach for the robust and stable numerical simulation of hybrid systems with chattering behavior, characterized either by infinite fast control actions or by discontinuous laws of physics. We have proposed a technique to detect chattering behavior "on the fly" in real-time simulation. Necessary and sufficient conditions driving to chattering behavior are explicitly introduced, and the treatment of chattering behavior during the numerical simulation using so-called sliding mode simulation is studied. A simulation algorithm is proposed that guarantees a robust treatment of chattering behavior. Its purpose is to organize mode switching and to allow sliding mode simulation each time the necessary and sufficient condition for chattering is satisfied. A novel computational framework which treats automatically any non-smoothness in the trajectory of the state variables during the regularization of the chattering path by a smooth correction after each integration time-step was also provided. The main objective of the computational algorithm is to switch between the transversality modes and the sliding modes simulation automatically as well as integrating each particular state appropriately and localize the structural changes in the system in an accurate way. Our approach is based on mixing compile-time transformations of hybrid programs (generating what is necessary to compute the smooth equivalent dynamics), the decision at runtime of the necessary and sufficient conditions for entering and exiting a sliding mode, and the computation, at runtime, of the smooth equivalent dynamics. We have shown by a special hierarchical application of convex combinations that unique solutions can be found in general cases when the switching function takes the form of finitely many intersecting manifolds so that an efficient numerical treatment of the sliding motion constrained on the entire discontinuity region (including the switching intersection) is guaranteed.

Finally, the simulation results - reported here on a set of representative case studies - showed that our approach is efficient and precise enough to provide a chattering bath avoidance, to perform a special numerical treatment of the constrained motion along the discontinuity surface, as well as its robustness in achieving an accurate detection and localization of the switch points for both entering to- and exiting from- the sliding region for the case of a single manifold of discointuniuity as well as the case of switching intersection.

Acknowledgements

This work was supported by the ITEA2/MODRIO project under contract N° 6892, and the ARED grant of the Brittany Regional Council.

References

Myron Allen and Eli Isaacson. Numerical analysis for applied science. *John Wiley and Sons*, 1998.

Klaus-Jürgen Bathe and Gunwoo Noh. Insight into an implicit time integration scheme for structural dynamics. *Computers and Structures*, 2012.

Albert Benveniste, Timothy Bourke, Benoit Caillaud, and Marc Pouzet. Non-standard semantics of hybrid systems modelers. *Journal of Computer and System Sciences*, 2012.

Martin Biák, Tomáš Hanus, and Drahoslava Janovská. Some applications of filippov's dynamical systems. *Journal of Computational and Applied Mathematics*, 2013.

John Charles Butcher. Numerical methods for ordinary differential equations. *John Wiley and Sons*, 2008.

Chaohong Cai, Rafal Goebel, Ricardo Sanfelice, and Andrew Teel. Hybrid systems: limit sets and zero dynamics with a view toward output regulation. *Springer-Verilag*, 2007.

François Cellier and Ernesto Kofman. Continuous system simulation. *Springer Verlag*, 2006.

Mario di Bernardo, Chris Budd, Alan Champneys, Piotr Kowalczyk, Arne Nordmark, Gerard Olivar Tost, and Petri Piiroinen. Bifurcations in nonsmooth dynamical systems. *Industrial and Applied Mathematics*, 2008.

Aleksei Fedorovich Filippov. Differential equations with discontinuous right-hand sides. *Mathematics and its Applications*, Kluwer Academic, 1988.

Marcel Guardia, Tere Seara, and Marco Antonio Teixeira. Generic bifurcations of low codimension of planar filippov systems. *Journal of Differential Equations*, 2011.

Karl Henrik Johansson, Andrey Barabanov, and Karl Johan Åström. Limit cycles with chattering in relay feedback systems. *IEEE TRANSACTIONS ON AUTOMATIC CONTROL*, 47(9), 2002.

Autar Kaw and Egwu Eric Kalu. Numerical methods with applications (1st edition). *WordPress.*, 2008.

Hai Lin and Panos J. Antsaklis. Hybrid dynamical systems: Stability and stabilization. *The Control Systems Handbook, Second Edition: Control System Advanced Methods. CRC Press*, 2009.

Ben Morris. Hybrid invariant manifolds in systems with impulse effects with application to periodic locomotion in bipedal robots. *IEEE Transactions on Automatic Control*, 2009.

Claus-Dieter Munz, Florian Hindenlang, and Gregor Gassner. A runge-kutta based discontinuous galerkin method with time accurate local time stepping. *Numerical Methods for Hyperbolic Equations: Theory an Applications.*, 2011.

Peter Schrammel. *Logico-Numerical Verification Methods for Discrete and Hybrid Systems*. PhD disseretation, 2012.

Vadim Utkin. Sliding mode in control and optimization. *Springer, Berlin*, 1992.

Daniel Weiss, Tassilo Küpper, and Hany Hosham. Invariant manifolds for nonsmooth systems with sliding mode. *Mathematics and Computers in Simulation*, 2014.

Fu Zhang, Murali Yeddanapudi, and Pieter Mosterman. Zero-crossing location and detection algorithms for hybrid system simulation. *IFAC W. Cong.*, 2008.

Jun Zhang, Karl Henrik Johansson, John Lygeros, and Shankar Sastry. Zeno hybrid systems. *International Journal of Robust and Nonlinear Control*, 2001.